A high-content drug screening strategy to identify protein level modulators for genetic diseases: a proof-of-principle in Autosomal Dominant LeukoDystrophy (ADLD)

A high-content drug screening strategy to identify protein levels modulators for rare genetic diseases: a proof-of-principle in Autosomal Dominant LeukoDystrophy (ADLD).

Elisa Giorgio[1,*], Emanuela Pesce[2,*], Elisa Pozzi[1], Elvira Sondo[2], Marta Ferrero[1], Giusy Borrelli[1], Edoardo Della Sala[1], Martina Lorenzati[3], Pietro Cortelli[4,5], Annalisa Buffo[3], Nicoletta Pedemonte[2,*], Alfredo Brusco[1,6,*].

[1] University of Torino, Department of Medical Sciences, Medical Genetics Unit, 10126, Turin, Italy
[2] UOC Genetica Medica, IRCCS Istituto Giannina Gaslini, 16147, Genova, Italy.
[3] University of Torino, Department of Neuroscience Rita Levi Montalcini and Neuroscience Institute Cavalieri Ottolenghi (NICO), Orbassano, 10043, Torino, Italy.
[4] University of Bologna, Department of Biomedical and Neuromotor Sciences, 40123, Bologna, Italy
[5] IRCCS Istituto delle Scienze Neurologiche di Bologna, Bellaria Hospital, 40139, Bologna, Italy.
[6] Medical Genetics Unit, Città della Salute e della Scienza University Hospital, 10126, Turin, Italy.

[*] These authors equally contributed to the work

Corresponding authors: Elisa Giorgio (elisa.giorgio@unito.it) and Alfredo Brusco (alfredo.brusco@unito.it), University of Torino, Department of Medical Sciences, via Santena 19, 10126, Torino, Italy. Fax +390112365926

Funding: The work was supported by the Fondazione Umberto Veronesi (post-doctoral fellowship 2017 to EG), Ricerca locale MURST ex 60% and the "Associazione E. E. Rulfo per la ricerca biomedica" to ABrusco. Ministero dell'Istruzione, dell'Università e della Ricerca – MIUR "Dipartimenti di Eccellenza 2018–2022" to Department of Medical Sciences (Project D15D18000410001). Work in NP lab was supported by the Jerome Lejeune Foundation (Project #1672/2017) and by the Italian Ministry of Health through Cinque per mille and Ricerca Corrente (Linea1).

Key words: pharmacological screening, ADLD, Lamin B1, rare disease, dosage-sensitive gene, therapy, alvespimycin.

ABSTRACT

In genetic diseases, the most prevalent mechanism of pathogenicity is an altered expression of dosage-sensitive genes. Drugs restoring their physiological levels are anticipated to be effective in treating the associated conditions. We developed a screening strategy, based on a bicistronic dual-reporter vector, able to identify compounds modulating proteins levels, and used it in a pharmacological screening approach. To provide a proof-of-principle, we chose Autosomal Dominant LeukoDystrophy (ADLD), an ultrarare adult-onset neurodegenerative disorder caused by Lamin B1 (LMNB1) overexpression. In our method, a stable CHO cell line simultaneously expresses an AcGFP reporter fused to LMNB1 and a Ds-Red normalizer. Using high-content imaging analysis, we screened a library of 717 biologically active compounds and approved drugs and identified alvespimycin, an HSP90 inhibitor, as positive hit. We confirmed alvespimycin could reduce LMNB1 levels by 30-80% in 5 different cell-lines (fibroblasts, NIH3T3, CHO, COS-7 and rat primary glial cells). In ADLD fibroblasts, the drug reduced cytoplasmic LMNB1 of ~50%. We propose our approach is effective to identify potential drugs for treating genetic diseases associated with deletions/duplications and pave the way towards a "compassionate use" of alvespimycin in ADLD.

INTRODUCTION

Orphan diseases are conditions affecting a small number of people compared to general population. The specific definition varies from country to country: in the United States, rare diseases are those with a prevalence < 1:200,000, whereas in Europe are disorders affecting < 1:2,000 individuals. Approximately 7,000 rare diseases have been identified and collectively they affect more than 350 million people worldwide (Govindaraj, Naderi, Singha, Lemoine, & Brylinski, 2018). A therapeutic option is available for only 5% of rare diseases (Xue, Li, Xie, & Wang, 2018) and due to extremely small individual markets, orphan diseases are of limited interest to the biopharmaceutical industry. Moreover, the price of treatment *per* patient is generally high because the cost of the drug discovery is shared by a small number of individuals. On that account, many countries passed orphan drug legislation to encourage drug development for rare diseases (Sun, Zheng, & Simeonov, 2017). These financial incentives together with the use of drug repositioning approaches allowed to strongly increase the number of FDA-approved drugs for rare diseases, signifying the importance of drug repositioning to orphan disease research.

Drug repositioning, often referred as "old drugs for new uses", is an effective, low-cost, and lower-risk strategy to find novel indications for existing drugs. This approach has several advantages: (i) to search for an effective compound among chemicals that have already passed safety tests, avoiding 30% of clinical trial failures due to harmful compounds; (ii) the drugs bioavailability and pharmacokinetics are known; (iii) the cost of producing a repositioned drug is limited if compared to that required for the discovery and development of a new drug; (iv) the translation into clinical practice will be faster. The effectiveness of such approach is testified by the fact that more than 30% of the new pharmacological products launched in recent years are line extensions of previously marketed compounds (Graul & Cruces, 2011; Graul, Cruces, Dulsat, Arias, & Stringer, 2012; Graul, Cruces, & Stringer, 2014; Graul, Navarro, Dulsat, Cruces, & Tracy, 2014; Graul et al., 2010), and

many successes have been reported through the years, among which amantadine for Parkinson disease (Paquette et al., 2012), topiramate for essential tremor (Ondo et al., 2006) and Tourette syndrome (Jankovic, Jimenez-Shahed, & Brown, 2010), and, very recently, lonaprisan in a mouse model of Pelizaeus-Merzbacher disease (Prukop et al., 2014) and celecoxib for prevention and treatment of colon, breast, prostate and head and neck cancers (Tołoczko-Iwaniuk, Dziemiańczyk-Pakieła, Nowaszewska, Celińska-Janowicz, & Miltyk, 2019). The success of drug-repositioning approaches is strongly related to the optimization of appropriate reporter cell lines and assays suitable for high-throughput screening (HTS).

Two major classes of *in vitro* assays are exploited for HTS: biochemical assays (measurements of enzyme activity, protein-protein and protein-DNA interactions) and cell-based assays using, in most cases, specifically-engineered cell lines (e.g., stably over-expressing a protein of interest, or designed to perform reporter-gene assays and second-messenger assays). These assays need to be miniaturized and optimized for large-scale screening of compounds, reaching a robustness suitable for HTS (Z' factor)(Zhang, Chung, & Oldenburg, 1999).

Even if genetic diseases are so heterogeneous, the molecular causes can be grouped into a handful of classes, and in most cases a gene dosage alteration takes place. For this reason, rare diseases that share a common molecular etiology could benefit from drug-repositioning approaches based on the same screening strategy. For instance, the identification of drugs restoring physiological protein levels represents a promising therapeutic approach for all genetic disorders associated with genomic deletions/duplications but also loss/gain of function mutations. An instructive example is Autosomal Dominant adult-onset demyelinating LeukoDystrophy (ADLD, OMIM#169500) (Eldridge et al., 1984) a slowly progressive neurodegenerative disease which occurs in the 4^{th}-5^{th} decade of life with autonomic symptoms, which can precede cerebellar and pyramidal abnormalities by several years. ADLD is caused by excessive Lamin B1 (LMNB1) production due to gene duplication (Giorgio et al., 2013; Padiath et al., 2006) or to alteration of the *LMNB1* regulatory landscape (Giorgio et al.,

2015; Nmezi et al., 2019). The pathogenic mechanisms underlying ADLD have only begun to be explored and directly involve LMNB1 overexpression and protein accumulation (Bartoletti-Stella et al., 2015; Giacomini, Mahajani, Ruffilli, Marotta, & Gasparini, 2016; Heng et al., 2013; Rolyan et al., 2015). It stands to reason that a drug able to restore physiological levels of LMNB1 mRNA/protein represents a promising strategy for treating ADLD (Giorgio et al., 2019; Lin & Fu, 2009). Indeed, ADLD is considered an ideal candidate for the identification of potential drugs, because patients have a homogenous pathogenetic basis, a relative slow-progression with an adult onset as highlighted recently by (Nmezi et al., 2020).

Here, we describe the development and validation of an innovative assay based on a dual-reporter cell line, designed for high-throughput screening of compounds libraries by high-content imaging and analysis to identify modulators of protein levels rapidly and efficiently. As a proof-of-principle, we exploited this cell line to perform a screening of an in-house library of 717 biologically active compounds, resulting in the identification of effective drugs reducing Lamin B1 levels as therapeutic option for ADLD.

MATERIALS AND METHODS

Generation of the dual-reporter plasmid (CAG-AcGFP-hLMNB1-IRES-DsRed)

We have designed a custom dual reporter backbone containing a CAG promoter, the green fluorescent protein (AcGFP) fused with the N-terminal of full-length cLMNB1, an internal ribosomal entry site (IRES) and the monomeric DsRed_Express2 (hereafter named DsRed) reporter gene (CAG-AcGFP-hLMNB1-IRES-DsRed; fig. 1-2 and supplemental fig.1). The DsRed reporter cassette is flanked by the *BamHI* and *NheI* unique restriction sites, to allow removal / substitution of the reporter for future applications. The generation of the plasmid was outsourced to VectorBuilder Inc. (Chicago, IL 60609, USA).

Generation of the stable dual-reporter cell lines for HTS

CHO (Chinese hamster ovary cell) cells were stable transfected with the reporter plasmid (CAG-AcGFP-hLMNB1-IRES-DsRed) carrying the resistance gene for puromycin. Cells were cultured in Ham's F-12 (1:1) medium supplemented with 10% fetal bovine serum (FBS), 2 mM L-glutamine, 100 U/ml penicillin, and 100 µg/ml streptomycin. Clones were evaluated for their stability of reporter proteins expression during at least 20 cell passages in 2 µg/ml puromycin-containing medium. Preliminary evaluation of reporter proteins expression was performed using a Nikon Eclipse Ti-E microscope-based high-content screening system.

For high-content assay primary screening, CHO cells were plated in a total volume of 100 µl of culture media (20,000/well) on high-quality 96-well clear-bottom black plates suitable for high-content imaging (Corning, Corning, NY, USA). Plates were then incubated at 37°C, 5% CO_2. After 24 hrs., cells were treated with test compounds at 5 µM for 24 hrs., unless otherwise indicated, and following 24 hrs., plates were assayed.

For high-content analysis of AcGFP-Lamin B1 signal texture, CHO cells were plated (10,000/well) on high-quality 96-well clear-bottom black plates. After incubation at 37°C, 5% CO_2 for 24 hrs., cells were treated with test compounds at the desired concentration for up to 72 hrs., during which plates were imaged every 24 hrs.

Immunofluorescence

Cells were plated onto coverslips, fixed in 4% PFA and immunolabeled as previously described (Giorgio *et al.*, 2019). Samples were immunostained using rabbit polyclonal anti-LMNB1 (ab16048, Abcam) and Alexa Fluor 488 goat anti-rabbit secondary antibody (Thermo Fisher Scientific, Waltham, MA, USA) or directly acquired (CHO dual-reporter cell line). The confocal optical sectioning was performed at room temperature (RT) using a Leica TCS SP5 AOBS TANDEM inverted confocal microscope that was equipped with a 40 × HCX PL APO 1.25 oil objective lens.

Library compounds and library screening

Master plates of the in-house library of 717 biologically active compounds were originally diluted at 10 mM in DMSO and stocked at -80°C until use. The complete list of compounds included in the library is provided in Supplemental Table 1. Working plates were prepared at 15 µM by diluting compounds from master plates in medium. Test compounds were then added to the cells at a final concentration of 5 µM, unless otherwise indicated.

High-content assay for determination of Lamin B1 expression level

To evaluate Lamin B1 expression level, at the end of treatment CHO cells were washed with D-PBS, then plates were imaged in non-confocal mode with a 10X air objective using the Opera Phenix (Perkin Elmer, Waltham, MA, USA) high-content screening system. AcGFP-Lamin B1 signal was laser-excited at 480 nm and the emission wavelengths were collected between 500 and 550 nm. DsRed_Express2 signal was laser-excited at 561 nm and the emission wavelengths were collected between 570 and 630 nm.

High-content analysis of AcGFP-Lamin B1 signal texture

To analyze AcGFP-Lamin B1 signal texture, after washing with D-PBS, plates were imaged in confocal mode with a 40X water-immersion objective using the Opera Phenix high-content screening system. AcGFP-Lamin B1 and DsRed_Express2 signals were excited and collected as described for determination of Lamin B1 expression levels.

Algorithm for automated image analysis

Automated image analysis was performed using the Harmony software (version 4.9) of the Opera Phenix high-content screening system, by means of automated algorithms, developed using machine-

learning techniques. The algorithm utilized for the determination of Lamin B1 expression level was based on the automatic recognition of cell nucleus, cell cytoplasm and plasma membrane based on AcGFP and DsRed_Express2 signal morphology and intensity.

The algorithm used for the analysis of AcGFP-Lamin B1 signal texture (describing the spatial arrangement of signal intensities in an image) was performed using the PhenoLogic machine-learning algorithm of the Harmony software and it was based on evaluation of Haralick and Gabor features, two subsets of well-known parameters (Haralick, Shanmugam, & Dinstein, 1973; Turner, 1986), and evaluation of SER (Spots, Edges, Ridges) features, developed by Perkin Elmer and included in the Harmony software of Opera Phenix.

DIRK1A and LMNB1 immunolocalization

Parental SH-SY5Y and SH-SY5Y cells stably overexpressing DYRK1A were cultured in Dulbecco's modified Eagle's / Ham's F-12 (1:1) medium supplemented with 10% FBS, 2 mM L-glutamine, 100 U/ml penicillin, and 100 µg/ml streptomycin. For immunolocalization of DYRK1A and LMNB1, cells were plated (30,000/well) on high-quality 96-well clear-bottom black plates. After incubation at 37°C, 5% CO_2 for 24 hrs., cells were treated with alvespimycin at the desired concentration for 24 hrs., after which cells were formalin-fixed and immunostained using rabbit polyclonal anti-DYRK1A (HPA015323, Sigma-Aldrich, St. Louis, MS, USA) or rabbit polyclonal anti-LMNB1 (HPA050524, Sigma-Aldrich, St. Louis, MS, USA) and Alexa Fluor 647 goat anti-rabbit secondary antibody (Thermo Fisher Scientific, Waltham, MA, USA). Cells were then imaged in confocal mode with a 40X water-immersion objective using the Opera Phenix high-content imaging system.

Cell culture and alvespimycin treatments.

Human control or ADLD fibroblasts, COS-7 (African green monkey kidney), CHO (Chinese hamster ovary cell) and NIH3T3 (mouse embryonic fibroblast) cell lines were cultured in DMEM with the

addition of 10% FBS. All cultures were incubated at 37°C in the presence of 5% CO_2. For alvespimycin treatment, cells were seeded at a concentration of $2x10^5$ cells/well in a 6-well plate and incubated for 24 hours in complete medium. Alvespimycin (SelleckChem, Munich, Germany) or DMSO (vehicle alone) were added to cell media at a final concentration of 5 μM or 10 μM.

Mixed glial cell cultures were obtained from P0-2 Sprague-Dawley rat cortex, as described previously (Boda et al., 2015), with slight modifications. Glial cells were plated at 90,000 cells/well onto poly-D-lysine (1 μg/mL, Sigma-Aldrich, Milan, Italy) coated Thermo Fisher 6-well plates and cultured in BME with 2mM L-glutamine and 10% Fetal Bovine Serum (FBS) for five days before alvespimycin treatment. At this stage cultures comprise a mixed population of astrocytes and oligodenroglial cells. Alvespimycin or DMSO (vehicle alone) were added to cell media at a final concentration of 1 μM, 5 μM or 10 μM.

Treated cells were harvested at twenty-four or thirty hours post treatment and processed to extract nuclear and cytoplasmic proteins using the NE-PER™ Nuclear and Cytoplasmic Extraction Reagents (Thermo Fisher Scientific). At least three biological replicates were performed for each tested cell line. A total of six or four fibroblast cell lines, from control or ADLD patients respectively, were treated with alvespimycin for 24 hrs. or 30 hrs.

Western blot analysis.

Four micrograms of nuclear protein extracts and 10 μg of cytoplasmic protein extracts were run on NuPAGE 4-12% Bis-tris Gel (Invitrogen, Thermo Fisher Scientific), then blotted onto nitro-cellulose (Bio-Rad, Hercules, CA, USA) in Tris/Glycine buffer with 20% methanol at 4°C for 90 min. Protein transfer efficiency was evaluated using the MemCode Reversible Protein Stain Kit (Pierce Biotechnology Rockford, IL, USA). Lamin B1 was detected using primary anti-lamin B1 (ab16048, Abcam, Cambridge, UK) antibody and WesternBreeze™ Chemiluminescent Detection Kit (Invitrogen, Thermo Fisher Scientific). Images were captured with a ChemiDoc™ XRS+ System and

densitometry analysis was performed with Image Lab™ Software (Bio-Rad).

Statistical Analysis.

The Kolmogorov-Smirnov test was used to evaluate the assumption of normality. Normally distributed data are expressed as means ± SEM. For normally distributed quantitative variables, the one-way parametric analysis of variance (ANOVA) was performed, followed by the Dunnet multiple post-hoc test to avoid multiple comparison errors when comparing more than two groups.

Graphics and statistical analysis were performed with GraphPad Prism version 5.00 (GraphPad software, San Diego, CA, USA). Data are presented as mean ± standard error of the mean (SEM). All data were analyzed using two-tailed Mann-Whitney t-test.

Editorial Policies and Ethical Considerations

Patients cells were obtained after informed consent; the study conforms to the standards of the Declaration of Helsinki and was approved by the Internal Review board at University of Torino.

RESULTS

Generation of a dual-reporter plasmid (CAG-AcGFP-hLMNB1-IRES-DsRed)

To identify modulators of LMNB1 protein levels, we generated a dual-reporter expression plasmid composed by an IRES-containing bicistronic vector allowing the simultaneous expression of two distinct proteins from the same RNA transcript: i) a chimeric protein, consisting at the N-terminal of the monomeric *Aequorea coerulescens* green fluorescent protein (AcGFP) fused with the full-length human lamin B1 (LMNB1). The AcGFP-LMNB1 construct was previously used to characterize the nuclear pore complex in living cells and to study LMNB1 overexpression-dependent cellular phenotypes. The chimeric protein showed the expected nuclear localization, physiological turnover and function (Daigle et al., 2001; Lin & Fu, 2009); ii) a destabilized red fluorescent protein (RFP),

the DsRed, having an shortened half-life of ~10 hours. Destabilized fluorescent proteins are constructed by fusing a fluorescent protein, to amino acid residues 422-461 of mouse ornithine decarboxylase, one of the most short-lived proteins in mammalian cells (Li et al., 1998). In our construct, a destabilized RFP allows a prompt readout for aspecific compounds modulating global transcription/translation rate. The rational was to discriminate compounds regulating target protein levels (specifically reducing green fluorescence) from those affecting transgene transcriptions or inhibiting global translation (affecting preferentially red fluorescence, given the short half-life of destabilized DsRed protein) (Fig. 1).

Generation of a stable dual-reporter cell line for HTS

To have a proof-of principle in the efficacy and utility of the CAG-AcGFP-LMNB1-IRES-DsRed dual-reporter plasmid for HTS, we transiently transfected HEK293T cells by lipofectamine, and analyzed red and green fluorescence at 12, 24, 36 and 48 hrs. using the Nikon Eclipse Ti-E microscope-based high-content screening system and by confocal microscopy (Fig. 2A). To verify whether the kinetic of DsRed disappearance in our system agreed with the reported half-life, we tested the expression of reporter proteins after protein translation blockage by cycloheximide. We observed a marked increase of the AcGFP/DsRed ratio (Fig. 2A), suggesting that destabilized RFP can promptly detect compounds affecting global translation rate.

The dual-reporter plasmid was used to generate a stable cell line suitable for HTS-based high-content imaging and analysis (Fig. 2B). As recipient cells, we used Chinese Hamster Ovary (CHO) cells because of their high proliferative capacity, strong substrate adhesion and optimal resolution in high-content imaging. Green fluorescence detection showed an intense and specific signal at the nuclear membrane, completely overlapping the physiological localization of the LMNB1 protein, and supporting a preserved function (Fig. 2B). Moreover, dual-reporter CHO cells showed nuclear anomalies resembling ADLD-specific blebs and invaginations detected in patients' cells (Fig.

2C)(Giorgio et al., 2019; Giorgio et al., 2015). Western blot analysis confirmed the expression of the endogenous Lamin B1 protein (~70 KDa) and the AcGFP-hLMNB1 chimeric protein (~100 KDa) specifically in stable dual-reporter cells (Fig. 2D).

Primary pharmacological screening to identify modulators of Lamin B1 protein level

We established optimal conditions to test for LMNB1 modulators with regards to CHO cell density at plating, culture, and timing for assay. The high-content assay for the identification of pharmacological compounds that modulate Lamin B1 protein level was performed using the Opera Phenix confocal high-content screening system (Perkin Elmer).

We screened an in-house library of 717 biologically active compounds which included kinase inhibitors, endocannabinoids, bioactive lipids, modulators of the autophagic pathway and Wnt signaling, and a set of orphan and FDA-approved drugs (complete list available in supplemental table 1). CHO stable reporter cells were plated (20,000/well) on high-quality 96-well clear-bottom black plates suitable for high-content imaging, in a total volume of 100 µl of culture media. After 24 hours, each tested compound was dispensed into individual wells at a volume to achieve the required final test concentration (5 µM). After additional 24 hours, plates were assayed.

Screening results are shown in figure 3. Control wells were constituted by reporter cells incubated with media containing vehicle alone (DMSO). For each compound/well, and for each cell in the field examined, we measured: i) AcGFP and DsRed fluorescence intensity (Fig. 3A and 3B); ii) AcGFP/DsRed ratio (Fig. 3C); and iii) cell count as a readout of cytotoxic effects of the compound tested (Fig. 3D). In the absence of a positive control compound able to reduce Lamin B1 expression, assay robustness for screening purposes was checked by determining the inter-plate and inter-day variability, presence of drift or edge effects, assay dynamic range, signal to background ratio and cell count. In addition, quality control metrics to detect abnormal changes in intensity, morphological, and textural measurements were implemented, based on a supervised machine-learning approach, to

highlight images that required visual inspection.

Under these control conditions, we used the DsRed signal intensity from single cells to normalize the overall variability of transcription / translation. For each compound tested, the AcGFP fluorescence intensity scores were then put into an ordered distribution (Fig. 3E). Figures 3F-H show the DsRed fluorescence intensity scores (Fig. 3F), the AcGFP/DsRed ratio scores (Fig. 3G) and cell count scores (Fig. 3H) using the same ranking order used for Fig. 3F, thus based on the ordered distribution of AcGFP fluorescence intensity. We considered as positive hits compounds whose cell AcGFP fluorescence intensity was lower than a threshold resulting from the average minus three standard deviations of cell AcGFP fluorescence intensity measured in vehicle-treated cells. The threshold corresponded to a 20% decrease in cell AcGFP fluorescence intensity as compared to DMSO-treated cells. Eighteen compounds, out of the 717 included in the library, significantly decreased cell AcGFP fluorescence intensity. However, only five significantly changed AcGFP/DsRed ratio. Three out of the 5 compounds were discarded because they also modulated significantly DsRed expression level, based on DsRed fluorescence intensity. A fourth compound was excluded because of cytotoxic effects, as evidenced by the markedly decreased cell count. Summarizing, the screening allowed us to identify one positive hit, alvespimycin, that significantly reduced AcGFP fluorescence intensity and AcGFP/DsRed ratio.

We evaluated the ability of alvespimycin to specifically decrease AcGFP fluorescence intensity at different concentrations. The compound was tested in the low and sub micromolar range on dual-reporter CHO cells (Fig. 4A). Alvespimycin was able to decrease cell AcGFP fluorescence intensity in a dose-dependent manner, with an EC50 of 3.2 μM and complete inhibition achieved at 10 μM (Fig. 4A). Because alvespimycin is a Heat Shock Protein 90 (HSP90) inhibitor, we also took in consideration two further HSP90 inhibitors: tanespimycin (17-AAG) or gedunin. These compounds were tested at different concentrations and the treatment with both drugs resulted in a dose-dependent decrease of cell AcGFP fluorescence intensity, in analogy with that observed upon treatment with

alvespimycin (Fig. 4B).

We monitored the effect of alvespimycin treatment on nuclear envelope morphology by means of high-content imaging and analysis of dual-reporter CHO cells. For this purpose, CHO cells were plated at low density on high-quality 96-well plates for imaging and, the following day, cells were treated with vehicle alone (DMSO) or alvespimycin at the desired concentrations. Cells were then imaged every 24 hrs. up to 72 hours. We performed a texture analysis of AcGFP-LMNB1 signal detected in cells under control condition (DMSO-treated) and following treatment with alvespimycin. Interestingly, alvespimycin significantly altered several parameters of AcGFP-LMNB1 signal texture in a dose-dependent manner, as calculated by Haralick's, Gabor and SER formulas (Supplemental Fig. 2).

Preliminary evaluation of alvespimycin specificity

We aimed to evaluate alvespimycin specificity for the normalization of Lamin B1 expression level, by testing its ability to regulate the expression of proteins, upregulated in a human disease because of genomic duplication, but unrelated to Lamin B1.

We chose the dual-specificity tyrosine phosphorylation-regulated kinase 1A (DYRK1A) encoded by a gene in the Down Syndrome (DS) critical region, a target we were presently studying in our laboratory for other projects. DYRK1A is overexpressed in DS patients and DS mouse models (Dowjat et al., 2007; Guimera, Casas, Estivill, & Pritchard, 1999), and it is involved in brain functions and processes altered in DS (Liu et al., 2008; Wegiel, Gong, & Hwang, 2011). We used an SH-SY5Y cell line stably overexpressing DYRK1A (SH-SY5Y DYRK1A clone 2; Supplemental fig. 3) and monitored DYRK1A levels by immunolocalization coupled to confocal imaging and analysis based fluorescent signal intensity (Fig. 5A). Treating cells with 5 μM alvespimycin - a concentration that is able to downregulate Lamin B1 - we did not detect any change in DYRK1A levels; notably, cells treated with higher doses of alvespimycin showed a dose-dependent increase in overall DYRK1A

expression, as compared to DMSO-treated control cells (1.6-fold at 10 μM alvespimycin; up to 2.7-fold at 20 μM alvespimycin; fig. 5A, B). We thus evaluated alvespimycin on SH-SY5Y parental cells, that have an endogenous DYRK1A expression, although lower than DYRK1A overexpressing cells (Fig. 5C). Interestingly, in these cells the ability of alvespimycin to increase overall DYRK1A expression was markedly reduced as compared to DYRK1A overexpressing cells (Fig. 5D). Immunodetection of LMNB1, however, demonstrated that nuclear content of this protein was reduced following treatment with alvespimycin (Fig. 5E, F).

Validation of alvespimycin activity in different cell types.

The ability of alvespimycin to reduce LMNB1 protein levels has been tested *in vitro* on five different cell lines, namely CHO, COS-7, NIH3T3, human fibroblasts and rat primary glial cells. Western blot analysis was performed on nuclear fraction (NF) and cytoplasmic fraction (CF) extracts of non-treated, treated with vehicle (DMSO) or with alvespimycin cells. We observed that the drug reduced LMNB1 protein in all cell lines at all concentrations tested with a stronger efficacy on the cytoplasmic fraction (Mean percentage of reduction at the highest concentration tested vs DMSO: NF: 47.7%; CF: 68.2%; fig. 6; supplemental table 2). Interestingly, the treatment of CHO-dual-reporter cells effectively reduced the amount of both the endogenous Lmnb1 and the human LMNB1-GFP protein expressed from the dual-reporter plasmid (mean percentage of reduction at the highest concentration tested vs DMSO [LmnB1; NF: 66.1%; CF: 68%];[hLMNB1-GFP; NF:73.2%; CF: 69.4%]; fig. 6; supplemental table 2).

As a final experiment, to preliminary evaluate the therapeutic potential of alvespimycin as treatment for ADLD, we evaluate the efficacy of the drug on human ADLD fibroblasts. The 24 hours treatment significantly reduced the cytoplasmic fraction (Mean percentage of reduction at the highest concentration tested vs DMSO: NF: 6%; CF: 47.6%; fig. 6; supplemental table 2); after 30 hours of treatment, both NF and CF were significantly reduced (mean percentage of reduction at the highest

concentration tested vs DMSO: NF: 40.3%; CF: 84.8%; fig. 6; supplemental table 2).

DISCUSSION

Rare genetic diseases affect a small number of patients each. Thus, they are of limited interest to the biopharmaceutical industry. Since the vast majority still have no treatment option, a cost-effective strategy is the repurposing of existing drugs as a therapy for new disorders. The success of drug-repositioning approaches is strongly related to the optimization of an appropriate reporter cell line suitable for high-throughput screening (HTS). We developed, optimized and validated an innovative dual reporter screening assay, based on an IRES-containing bicistronic vector, allowing the simultaneous expression of two distinct proteins from the same RNA transcript and therefore able to detect modulators specifically acting at protein level (translationally or post-translationally).

The identification of drugs restoring physiological protein levels represents a promising therapeutic strategy for many genetic disorders associated with genomic deletions/duplications. An instructive example is Autosomal Dominant LeukoDystrophy (ADLD), a rare disease caused by LMNB1 accumulation due to gene duplication or to a regulatory alteration (Giorgio et al., 2015; Giorgio et al., 2013; Nmezi et al., 2019), where the reduction of LaminB1 protein levels represents a promising strategy for treating ADLD patients (Giorgio et al., 2019). We fused the target gene (*LMNB1*) to a GFP reporter, and we included a second RFP reporter as normalizer. The resulting vector was exploited to generate a stable dual-reporter CHO cell line. This system can easily discriminate compounds specifically regulating the target protein levels, LMNB1 in our case, from those acting aspecifically, i.e. affecting transgene transcription or inhibiting global translation. The former cause a change in GFP amounts (green fluorescence), whereas the latter affect RFP (red fluorescence), which gives a prompt response given the shorter half-life of destabilized DsRed-Express2 RFP protein (Fig. 1).

The plasmid was used to generate a CHO stable cell line, which was critical for the screening, since

it is important to have i) a stable expression of the dual reporter, ii) an easy-to-grow cell line, iii) a simple cell morphology easy to be imaged. Using this system, we screened a library of 717 biologically active compounds by high-content HTS and have identified a positive hit in alvespimycin. This compound significantly reduced AcGFP fluorescence intensity and AcGFP/DsRed ratio, without affecting DsRed signal or cell growth.

Alvespimycin, alias 17-(dimethylaminoethylamino)-17-demethoxy-geldanamycin (17-DMAG), is a derivative of geldanamycin and a known heat shock protein 90 (Hsp90) inhibitor (Tian et al., 2004). Hsp90 is a chaperone that assists other proteins to fold properly, stabilizes proteins and aids in protein degradation (Schopf, Biebl, & Buchner, 2017). When the function of Hsp90 is inhibited, its client proteins are degraded leading to their depletion (Schopf et al., 2017). Besides alvespimycin, we also took into consideration other two compounds known to act as Hsp90 inhibitors, namely tanespimycin and gedunin. Tanespimycin is a benzoquinone geldanamycin structural analog, also known as 17-N-allylamino-17-demethoxygeldanamycin (17-AAG)(Erlichman, 2009), whereas gedunin is a pentacyclic triterpenoid compound, thus structurally unrelated to geldanamycin. Both drugs showed a dose-dependent reduction of AcGFP fluorescence, like that observed upon treatment with alvespimycin. These results suggest that modulation of LMNB1 more likely depends on their biological activity and is not a secondary effect due to their chemical structures. Thus, we hypothesize that Hsp90 inhibition negatively impact LMNB1 levels. Further studies will be necessary to understand whether Hsp90 plays a direct role in LMNB1 folding or degradation, or whether this effect occurs more indirectly, through modulation of other proteins that regulate LMNB1 protein levels.

Alvespimycin has been used in trials as an antitumor agent for solid tumors (Kummar et al., 2010; Pacey et al., 2011). Compared to other geldanamycin derivates, it exhibits some pharmacologically desirable properties such as reduced metabolic liability, lower plasma protein binding, increased water solubility, higher oral bioavailability, and reduced hepatotoxicity (DrugBank database; https://www.drugbank.ca/drugs/DB12442).

To validate the activity of alvespimycin, we tested the compound on five different cell lines (CHO, NIH3T3, COS7, human fibroblast and primary rat glial cells), confirming its ability to specifically reduce LMNB1 levels by western blot analysis on nuclear (mean reduction 47.7%) and cytoplasmic (mean reduction 68.2%) protein fractions. Interestingly, cytoplasmic LaminB1 protein is more affected by drug treatment. A possible explanation could be the different dynamism of the cytoplasmic fraction compared to the nuclear one (Dittmer & Misteli, 2011). The first represents the newly synthesized protein which is rapidly transported to the nucleus (Lehner, Furstenberger, Eppenberger, & Nigg, 1986) and which is therefore quickly modulated by the drug. The nuclear protein fraction, on the other hand, is much more stable especially once integrated into the nuclear lamina (Dittmer & Misteli, 2011) and for this reason its modulation may require longer treatment times. Also the different amount of Lamina B1 protein present in the cytoplasmic fraction (about 10%) compared to the nuclear one (90%) could explain the different efficacy of the treatment, making the drug-mediated reduction more visible in the fraction physiologically having a smaller amount of protein. Finally, the doubling time of the tested cell lines could also influence the different efficacy of the drug.

Indeed, alvespimycin treatment of ADLD primary fibroblasts (doubling-time greater than 24 hrs.) showed the lowest overall LaminB1 reduction, especially in the nuclear fraction (mean reduction 25.7%). On the other hand, rat primary glial cells showed a strong reduction of LMNB1 protein amount following the treatment, particularly in the nucleus (mean reduction: 87.4%). Among glial cells, oligodendrocyte progenitors display particularly high LMNB1 nuclear levels (Takamori et al., 2018) and mature oligodendrocytes are very sensitive to changes in the levels of LMNB1 that regulates several pathways, for example the synthesis of lipids (which make up 70% of myelin) (Rolyan et al., 2015) and the expression of proteolipid protein 1 (Plp1)(Heng et al., 2013), a transmembrane protein which represents the main component of myelin. Moreover, the increase in LMNB1 level induces the premature arrest of oligodendrocytes differentiation (Lin & Fu, 2009),

corroborating the key function of LMNB1 in glial cells. Such tight regulation of LMNB1 protein cellular levels may be linked to the observed glial sensitivity to pharmacological modulation of LMNB1 expression. Further studies on alvespimycin and its mechanism will be necessary to shed light on this hypothesis.

As a preliminary evaluation of alvespimycin specificity, we investigated its effect on DYRK1A expression level, as an unrelated target, overexpressed in DS. Interestingly, alvespimycin was not effective on SH-SY5Y cells having endogenous DYRK1A expression, while it caused an increase in DYRK1A expression in SH-SY5Y overexpressing DYRK1A. This suggests that pharmacological modulation of the expression levels of target proteins may vary not only according the biology of the target, but also depending on its expression level, since it could influence its cellular processing.

Finally, to evaluate the therapeutic relevance of alvespimycin on a pathology-relevant cell model, we tested alvespimycin on fibroblasts derived from ADLD patients. Interestingly, 24 hrs. treatment with alvespimycin caused a 50 % reduction of cytoplasmic LMNB1 protein, with no apparent effect on the nuclear fraction. However, when the treatment was prolonged up to 30 hours, we could detect a reduction of nuclear LMNB1 protein of about 40% in patients' cells, suggesting the existence of a fine tuning and possible feedbacks between cytoplasmic and nuclear fractions of LMNB1 protein.

In conclusion, our work describes an innovative dual-reporter plasmid allowing the identification of modulators acting specifically at protein level and the generation, optimization, and validation of a stable dual-reporter cell lines suitable for HTS. This strategy can be applied for the repositioning of exiting drugs, an approach that is expected to play a major role in the development of treatments for orphan diseases. The effectiveness of our strategy was testified by the identification of alvespimycin as modulator of LMNB1 protein levels. Our results may pave the way towards a clinical trial for ADLD following the "compassionate use" practice. Moreover, our dual reporter screening assay can be exploited to identify effective drugs for other genetic and multifactorial disorders in which the

modulation of a protein represents a promising therapeutic option, supporting the translational value of our research.

ACKNOWLEDGEMENTS

We thank patients and their families participating in the study.

DATA AVAILABILITY STATEMENT

Data available on request from the authors.

LEGENDS TO FIGURES

Figure 1. Overview for the dual-reporter strategy in a pharmacological screening.

A) Schematic representation of the innovative dual-reporter IRES-containing bicistronic vector allowing the simultaneous expression of a target and a reference protein from the same RNA transcript. The vector contains a CAG promoter followed by a fusion gene encoding the green fluorescent protein (AcGFP) joined to the N-terminal of the target protein; an internal ribosomal entry site (IRES) and the DsRed_Express2 reporter gene (CAG-AcGFP-cTARGET-IRES-DsRed). The synthesis of a target and reference protein by the same transcript allows to discriminate compounds regulating target protein levels (varying only green fluorescence) from those affecting transgene transcriptions or inhibiting global translation (modulating both green and red fluorescence). B-C) Rationale in the stable dual-reporter cell line suitable for high throughput screening of compounds libraries based on high-content imaging and analysis. Negative hits are drugs not affecting GFP/DsRED ratio. Panel B: strategy to identify compounds reducing target protein levels in gene dosage gain diseases. Positive hits are compounds reducing GFP/DsRED ratio, namely drugs specifically reducing GFP fluorescence. Panel C: strategy to identify compounds increasing target protein levels in gene dosage loss diseases. Positive hits are compounds increasing GFP/DsRED ratio, namely specifically increasing GFP fluorescence.

Figure 2. Validation of the dual-reporter vector and generation of a CHO stable dual-reporter cell line.

A) Schematic representation of the dual-reporter vector allowing the identification of Lamin B1 modulators (CAG-AcGFP-hLMNB1-IRES-DsRed). Confocal images of HEK293T cells transiently transfected with the plasmid. Red and green fluorescence were detected at 12, 24, 36 and 48 hrs. post transfection by confocal microscopy. Green fluorescence detection showed an intense and specific signal at the nuclear membrane completely overlapping the physiological localization of the LMNB1

protein, corroborating the preservation of LMNB1 function. Kinetics of DsRed-RFP disappearance in our system was evaluated by adding cycloheximide (CHX) to the medium for three hours. A marked increase of the GFP/RFP ratio was measured after cycloheximide treatment, suggesting that destabilized RFP can promptly detect compounds affecting overall translation rate and supporting the appropriateness of the dual reporter construct for the HTS. B) CHO stable dual reporter cell line shows the expression of both green and red plasmid-encoded proteins. Green fluorescence (GFP-LMNB1) strongly marked nuclear membrane, demonstrating the physiological localization of human LMNB1 protein. A 2-fold magnified inset is shown on the right (green filter). C) Nuclear shape was evaluated by fluorescent microscopy on wild-type (after LMNB1 staining) and stable dual-reporter CHO cell line. Nuclear abnormalities resembling ADLD-specific blebs and invaginations are clearly visible in the stable cell line. D) Evaluation of total LMNB1 protein by western blot (LMNB1 vs Memcode staining) in wild-type and stable dual-reporter CHO cell lines. Endogenous Lmnb1(about 70 KDa) protein is visible in both lines; GFP- human Lamin B1 recombinant protein (GFP-hLMNB1, about 100 KDa) is visible in stable dual-reporter cells only.

Figure 3. Drug-screening to identify modulators of LMNB1 expression level.

Figure shows results of the compound library screening performed on stable dual-reporter CHO cells. In panels A-D, each dot reports the measure of fluorescence intensity (A-C) or cell number (D) after 24-hr incubation with a different pharmacological compound (colored/black dots) or DMSO alone (negative control, grey dots). Panels A and B show the measure of green and red fluorescence, and panel C their ratio; positive hits are compounds able to reduce the GFP fluorescence leaving unaltered the DsRed fluorescence (see circles).

In E, decreasing ordered distribution of cell GFP fluorescence intensity measured, for each test compound, in the screening and displayed in A. F, G and H. Distribution of cell DsRed fluorescence intensity (F), GFP/DsRed fluorescence intensity ratio (G), cell count (H) measured in the screening

and displayed using the test compound ranking order determined in E.

Figure 4. Alvespimycin and other Hsp90 inhibitors decrease LMNB1 expression level.

A) Dose-response relationships of alvespimycin on cell GFP fluorescence intensity and DsRed fluorescence intensity, following 24 hrs. treatment on dual-reporter CHO cells. B). Dose-response relationships of tanespimycin (17-AAG; upper panels) and gedunin (lower panels) on cell GFP fluorescence intensity and DsRed fluorescence intensity, following 24 hrs. treatment on dual-reporter CHO cells. Mean ± SEM, n = 6. Asterisks indicate statistical significance versus the corresponding control (DMSO-treated cells): $p<0.05$: *; $p<0.01$: **.

Figure 5. Evaluation of alvespimycin specificity to modulate LMNB1 expression.

A) Representative images of DYRK1A immunolocalization in SH-SY5Y cells stably overexpressing DYRK1A, after treatment with the indicated concentration of alvespimycin for 24 hrs. B) Bar graph showing the quantification of DYRK1A protein in experiments described in A. C) Representative images of DYRK1A immunolocalization in parental SH-SY5Y cells, after treatment with the indicated concentration of alvespimycin for 24 hrs. D. Quantification of DYRK1A protein in experiments described in C. E. Representative images of LMNB1 immunolocalization in parental SH-SY5Y cells, after treatment with the indicated concentration of alvespimycin for 24 hrs. F. Quantification of LMNB1 protein in experiments described in E. Asterisks indicate statistical significance versus the corresponding control (DMSO-treated cells): **, $p < 0.01$; *, $p < 0.05$. Scale bar, 25 μm.

Figure 6. Validation of alvespimycin efficacy in five different cell lines and in ADLD fibroblasts.

Western blot analysis on nuclear (NF) and cytoplasmic (CF) extracts of non-treated, treated with vehicle (DMSO) or with alvespimycin (Alv) cells. Immunostaining with anti-LMNB1 antibody and

Memcode staining are shown as exemplification for CHO dual-reporter cell line and ADLD fibroblasts. Fold-change densitometric data and SEM are shown as bar plots. Statistically significant differences (asterisks) is reported for alvespimycin vs. corresponding DMSO treatment ($p<0.05$: *; $p<0.01$: **; two-tailed, Mann-Whitney test). Complete statistical analysis is reported in supplemental table 2. Protein marker: ProSieveTM QuadColor™ protein marker, 4.6 kDa – 300 kDa (Lonza).

REFERENCES

Bartoletti-Stella, A., Gasparini, L., Giacomini, C., Corrado, P., Terlizzi, R., Giorgio, E., . . . Capellari, S. (2015). Messenger RNA processing is altered in autosomal dominant leukodystrophy. *Hum Mol Genet, 24*(10), 2746-2756. doi:ddv034 [pii] 10.1093/hmg/ddv034

Boda, E., Di Maria, S., Rosa, P., Taylor, V., Abbracchio, M. P., & Buffo, A. (2015). Early phenotypic asymmetry of sister oligodendrocyte progenitor cells after mitosis and its modulation by aging and extrinsic factors. *Glia, 63*(2), 271-286. doi:10.1002/glia.22750

Daigle, N., Beaudouin, J., Hartnell, L., Imreh, G., Hallberg, E., Lippincott-Schwartz, J., & Ellenberg, J. (2001). Nuclear pore complexes form immobile networks and have a very low turnover in live mammalian cells. *J Cell Biol, 154*(1), 71-84.

Dittmer, T. A., & Misteli, T. (2011). The lamin protein family. *Genome Biol, 12*(5), 222. doi:gb-2011-12-5-222 [pii] 10.1186/gb-2011-12-5-222

Dowjat, W. K., Adayev, T., Kuchna, I., Nowicki, K., Palminiello, S., Hwang, Y. W., & Wegiel, J. (2007). Trisomy-driven overexpression of DYRK1A kinase in the brain of subjects with Down syndrome. *Neurosci Lett, 413*(1), 77-81. doi:10.1016/j.neulet.2006.11.026

Eldridge, R., Anayiotos, C. P., Schlesinger, S., Cowen, D., Bever, C., Patronas, N., & McFarland, H. (1984). Hereditary adult-onset leukodystrophy simulating chronic progressive multiple sclerosis. *N Engl J Med, 311*(15), 948-953. doi:10.1056/NEJM198410113111504

Erlichman, C. (2009). Tanespimycin: the opportunities and challenges of targeting heat shock protein 90. *Expert Opin Investig Drugs, 18*(6), 861-868. doi:10.1517/13543780902953699

Giacomini, C., Mahajani, S., Ruffilli, R., Marotta, R., & Gasparini, L. (2016). Lamin B1 protein is required for dendrite development in primary mouse cortical neurons. *Mol Biol Cell, 27*(1), 35-47. doi:10.1091/mbc.E15-05-0307

Giorgio, E., Lorenzati, M., Rivetti di Val Cervo, P., Brussino, A., Cernigoj, M., Della Sala, E., . . . Brusco, A. (2019). Allele-specific silencing as treatment for gene duplication disorders: proof-of-principle in autosomal dominant leukodystrophy. *Brain, 142*(7), 1905-1920. doi:10.1093/brain/awz139

Giorgio, E., Robyr, D., Spielmann, M., Ferrero, E., Di Gregorio, E., Imperiale, D., . . . Brusco, A. (2015). A large genomic deletion leads to enhancer adoption by the lamin B1 gene: a second path to autosomal dominant adult-onset demyelinating leukodystrophy (ADLD). *Hum Mol Genet, 24*(11), 3143-3154. doi:10.1093/hmg/ddv065

Giorgio, E., Rolyan, H., Kropp, L., Chakka, A. B., Yatsenko, S., Di Gregorio, E., . . . Padiath, Q. S. (2013). Analysis of LMNB1 duplications in autosomal dominant leukodystrophy provides insights into duplication mechanisms and allele-specific expression. *Hum Mutat, 34*(8), 1160-1171. doi:10.1002/humu.22348

Govindaraj, R. G., Naderi, M., Singha, M., Lemoine, J., & Brylinski, M. (2018). Large-scale computational drug repositioning to find treatments for rare diseases. *NPJ Syst Biol Appl, 4*, 13. doi:10.1038/s41540-018-0050-7

Graul, A. I., & Cruces, E. (2011). The year's new drugs & biologics, 2010. *Drugs Today (Barc), 47*(1), 27-51. doi:1587820 [pii] 10.1358/dot.2011.47.1.1587820

Graul, A. I., Cruces, E., Dulsat, C., Arias, E., & Stringer, M. (2012). The year's new drugs & biologics, 2011. *Drugs Today (Barc), 48*(1), 33-77. doi:1769676 [pii] 10.1358/dot.2012.48.1.1769676

Graul, A. I., Cruces, E., & Stringer, M. (2014). The year's new drugs & biologics, 2013: Part I. *Drugs Today (Barc), 50*(1), 51-100. doi:2116673 [pii] 10.1358/dot.2014.50.1.2116673

Graul, A. I., Navarro, D., Dulsat, C., Cruces, E., & Tracy, M. (2014). The year's new drugs & biologics, 2013: Part II. *Drugs Today (Barc), 50*(2), 133-158. doi:2122810 [pii] 10.1358/dot.2014.50.2.2122810

Graul, A. I., Sorbera, L., Pina, P., Tell, M., Cruces, E., Rosa, E., . . . Revel, L. (2010). The Year's New Drugs & Biologics - 2009. *Drug News Perspect, 23*(1), 7-36. doi:1440373 [pii] 10.1358/dnp.2010.23.1.1440373

Guimera, J., Casas, C., Estivill, X., & Pritchard, M. (1999). Human minibrain homologue (MNBH/DYRK1): characterization, alternative splicing, differential tissue expression, and overexpression in Down syndrome. *Genomics, 57*(3), 407-418. doi:10.1006/geno.1999.5775

Haralick, R. M., Shanmugam, K., & Dinstein, I. (1973). Textural Features for Image Classification. *IEEE Trans Systems Man Cybern, SMC-3*(6), 12.

Heng, M. Y., Lin, S. T., Verret, L., Huang, Y., Kamiya, S., Padiath, Q. S., . . . Fu, Y. H. (2013). Lamin B1 mediates cell-autonomous neuropathology in a leukodystrophy mouse model. *J Clin Invest, 123*(6), 2719-2729. doi:66737 [pii] 10.1172/JCI66737

Jankovic, J., Jimenez-Shahed, J., & Brown, L. W. (2010). A randomised, double-blind, placebo-controlled study of topiramate in the treatment of Tourette syndrome. *J Neurol Neurosurg Psychiatry, 81*(1), 70-73. doi:jnnp.2009.185348 [pii] 10.1136/jnnp.2009.185348

Kummar, S., Gutierrez, M. E., Gardner, E. R., Chen, X., Figg, W. D., Zajac-Kaye, M., . . . Murgo, A. J. (2010). Phase I trial of 17-dimethylaminoethylamino-17-demethoxygeldanamycin (17-DMAG), a heat shock protein inhibitor, administered twice weekly in patients with advanced malignancies. *Eur J Cancer, 46*(2), 340-347. doi:10.1016/j.ejca.2009.10.026

Lehner, C. F., Furstenberger, G., Eppenberger, H. M., & Nigg, E. A. (1986). Biogenesis of the nuclear lamina: in vivo synthesis and processing of nuclear protein precursors. *Proc Natl Acad Sci U S A, 83*(7), 2096-2099.

Li, X., Zhao, X., Fang, Y., Jiang, X., Duong, T., Fan, C., . . . Kain, S. R. (1998). Generation of destabilized green fluorescent protein as a transcription reporter. *J Biol Chem, 273*(52), 34970-34975. doi:10.1074/jbc.273.52.34970

Lin, S. T., & Fu, Y. H. (2009). miR-23 regulation of lamin B1 is crucial for oligodendrocyte development and myelination. *Dis Model Mech, 2*(3-4), 178-188.

Liu, F., Liang, Z., Wegiel, J., Hwang, Y. W., Iqbal, K., Grundke-Iqbal, I., . . . Gong, C. X. (2008). Overexpression of Dyrk1A contributes to neurofibrillary degeneration in Down syndrome. *FASEB J, 22*(9), 3224-3233. doi:10.1096/fj.07-104539

Nmezi, B., Giorgio, E., Raininko, R., Lehman, A., Spielmann, M., Koenig, M. K., . . . Padiath, Q. S. (2019). Genomic deletions upstream of lamin B1 lead to atypical autosomal dominant leukodystrophy. *Neurol Genet, 5*(1), e305. doi:10.1212/nxg.0000000000000305

Nmezi, B., Vollmer, L. L., Shun, T. Y., Gough, A., Rolyan, H., Liu, F., . . . Vogt, A. (2020). Development and Optimization of a High-Content Analysis Platform to Identify Suppressors of Lamin B1 Overexpression as a Therapeutic Strategy for Autosomal Dominant Leukodystrophy. *SLAS Discov*, 2472555220915821. doi:10.1177/2472555220915821

Ondo, W. G., Jankovic, J., Connor, G. S., Pahwa, R., Elble, R., Stacy, M. A., . . . Hulihan, J. F. (2006). Topiramate in essential tremor: a double-blind, placebo-controlled trial. *Neurology, 66*(5), 672-677. doi:01.wnl.0000200779.03748.0f [pii] 10.1212/01.wnl.0000200779.03748.0f

Pacey, S., Wilson, R. H., Walton, M., Eatock, M. M., Hardcastle, A., Zetterlund, A., . . . Judson, I. (2011). A phase I study of the heat shock protein 90 inhibitor alvespimycin (17-DMAG) given intravenously to patients with advanced solid tumors. *Clin Cancer Res, 17*(6), 1561-1570. doi:10.1158/1078-0432.CCR-10-1927

Padiath, Q. S., Saigoh, K., Schiffmann, R., Asahara, H., Yamada, T., Koeppen, A., . . . Fu, Y. H. (2006). Lamin B1 duplications cause autosomal dominant leukodystrophy. *Nat Genet, 38*(10), 1114-1123. doi:ng1872 [pii] 10.1038/ng1872

Paquette, M. A., Martinez, A. A., Macheda, T., Meshul, C. K., Johnson, S. W., Berger, S. P., & Giuffrida, A. (2012). Anti-dyskinetic mechanisms of amantadine and dextromethorphan in

the 6-OHDA rat model of Parkinson's disease: role of NMDA vs. 5-HT1A receptors. *Eur J Neurosci, 36*(9), 3224-3234. doi:10.1111/j.1460-9568.2012.08243.x

Prukop, T., Epplen, D. B., Nientiedt, T., Wichert, S. P., Fledrich, R., Stassart, R. M., . . . Sereda, M. W. (2014). Progesterone antagonist therapy in a Pelizaeus-Merzbacher mouse model. *Am J Hum Genet, 94*(4), 533-546. doi:S0002-9297(14)00103-7 [pii] 10.1016/j.ajhg.2014.03.001

Rolyan, H., Tyurina, Y. Y., Hernandez, M., Amoscato, A. A., Sparvero, L. J., Nmezi, B. C., . . . Padiath, Q. S. (2015). Defects of Lipid Synthesis Are Linked to the Age-Dependent Demyelination Caused by Lamin B1 Overexpression. *J Neurosci, 35*(34), 12002-12017. doi:10.1523/jneurosci.1668-15.2015

Schopf, F. H., Biebl, M. M., & Buchner, J. (2017). The HSP90 chaperone machinery. *Nat Rev Mol Cell Biol, 18*(6), 345-360. doi:10.1038/nrm.2017.20

Sun, W., Zheng, W., & Simeonov, A. (2017). Drug discovery and development for rare genetic disorders. *Am J Med Genet A, 173*(9), 2307-2322. doi:10.1002/ajmg.a.38326

Takamori, Y., Hirahara, Y., Wakabayashi, T., Mori, T., Koike, T., Kataoka, Y., . . . Yamada, H. (2018). Differential expression of nuclear lamin subtypes in the neural cells of the adult rat cerebral cortex. *IBRO Rep, 5*, 99-109. doi:10.1016/j.ibror.2018.11.001

Tian, Z. Q., Liu, Y., Zhang, D., Wang, Z., Dong, S. D., Carreras, C. W., . . . Myles, D. C. (2004). Synthesis and biological activities of novel 17-aminogeldanamycin derivatives. *Bioorg Med Chem, 12*(20), 5317-5329. doi:10.1016/j.bmc.2004.07.053

Tołoczko-Iwaniuk, N., Dziemiańczyk-Pakieła, D., Nowaszewska, B. K., Celińska-Janowicz, K., & Miltyk, W. (2019). Celecoxib in Cancer Therapy and Prevention - Review. *Curr Drug Targets, 20*(3), 302-315. doi:10.2174/1389450119666180803121737

Turner, M. R. (1986). Texture discrimination by Gabor functions. *Biol Cybern, 55*(2-3), 71-82.

Wegiel, J., Gong, C. X., & Hwang, Y. W. (2011). The role of DYRK1A in neurodegenerative diseases. *FEBS J, 278*(2), 236-245. doi:10.1111/j.1742-4658.2010.07955.x

Xue, H., Li, J., Xie, H., & Wang, Y. (2018). Review of Drug Repositioning Approaches and Resources. *Int J Biol Sci, 14*(10), 1232-1244. doi:10.7150/ijbs.24612

Zhang, J. H., Chung, T. D., & Oldenburg, K. R. (1999). A Simple Statistical Parameter for Use in Evaluation and Validation of High Throughput Screening Assays. *J Biomol Screen, 4*(2), 67-73.

Figure 1.

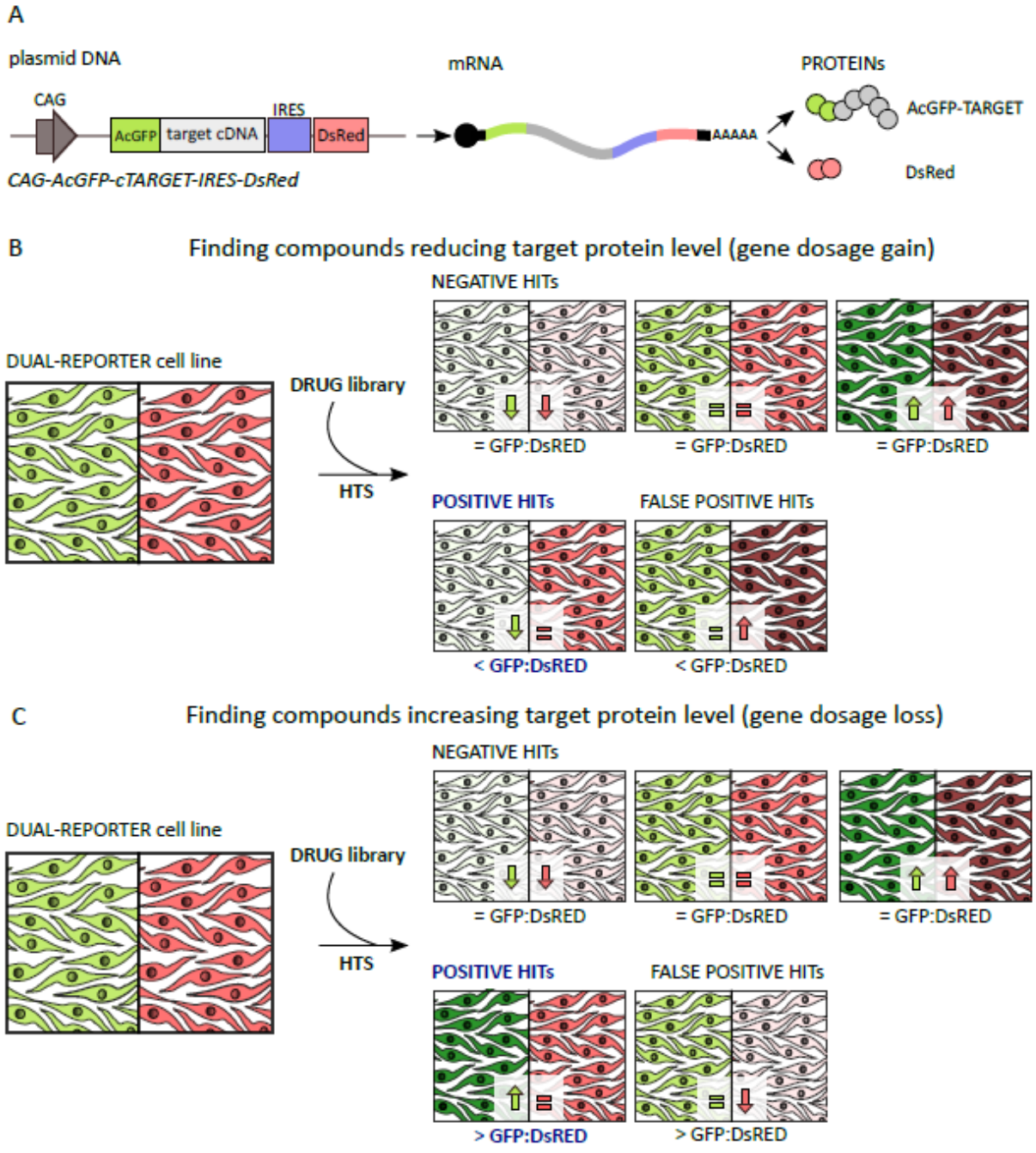
A
plasmid DNA
CAG
AcGFP
target cDNA
IRES
DsRed
CAG-AcGFP-cTARGET-IRES-DsRed
mRNA
AAAAA
PROTEINs
AcGFP-TARGET
DsRed
B
Finding compounds reducing target protein level (gene dosage gain)
DUAL-REPORTER cell line
DRUG library
HTS
NEGATIVE HITs
= GFP:DsRED
= GFP:DsRED
= GFP:DsRED
POSITIVE HITs
FALSE POSITIVE HITs
< GFP:DsRED
< GFP:DsRED
C
Finding compounds increasing target protein level (gene dosage loss)
DUAL-REPORTER cell line
DRUG library
HTS
NEGATIVE HITs
= GFP:DsRED
= GFP:DsRED
= GFP:DsRED
POSITIVE HITs
FALSE POSITIVE HITs
> GFP:DsRED
> GFP:DsRED

Figure 2.

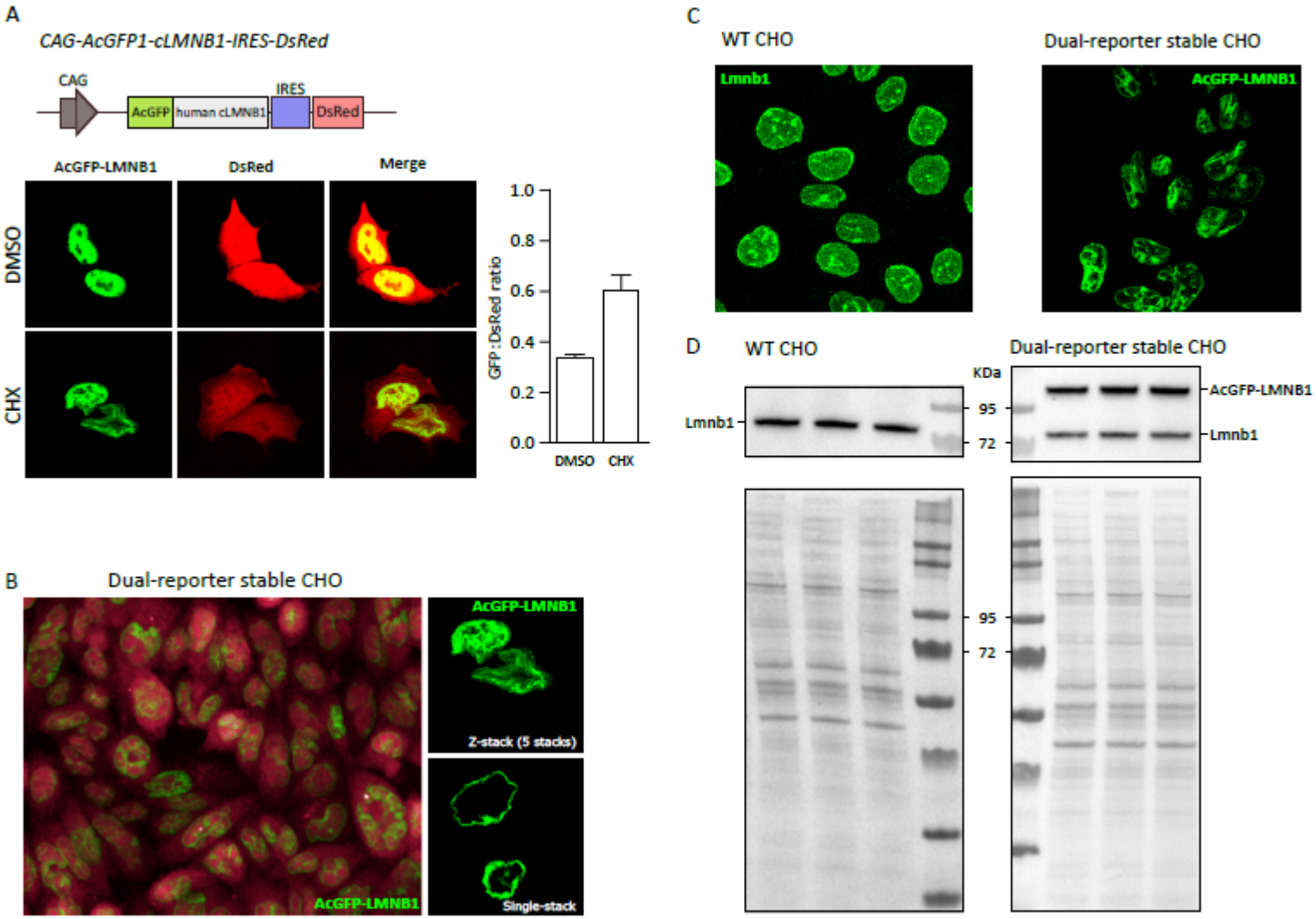
A
CAG-AcGFP1-cLMNB1-IRES-DsRed
CAG
IRES
AcGFP
human cLMNB1
DsRed
AcGFP-LMNB1
DsRed
Merge
DMSO
CHX
GFP:DsRed ratio
1.0
0.8
0.6
0.4
0.2
0.0
DMSO
CHX
B
Dual-reporter stable CHO
AcGFP-LMNB1
Z-stack (5 stacks)
AcGFP-LMNB1
Single-stack
C
WT CHO
Dual-reporter stable CHO
Lmnb1
AcGFP-LMNB1
D
WT CHO
Dual-reporter stable CHO
KDa
Lmnb1
95
72
AcGFP-LMNB1
Lmnb1
95
72

Figure 3.

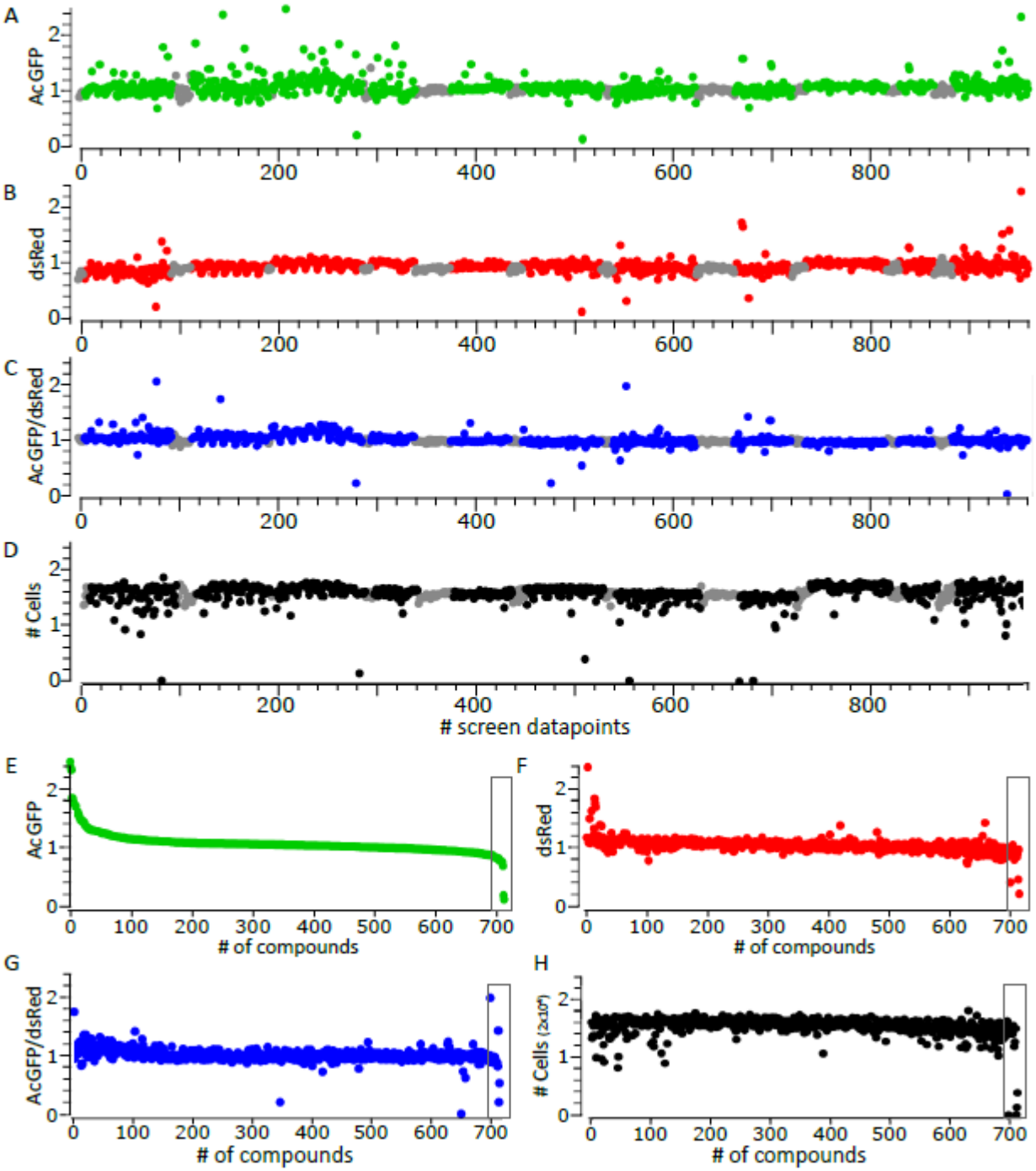
A
AcGFP
B
dsRed
C
AcGFP/dsRed
D
Cells
screen datapoints
E
AcGFP
# of compounds
F
dsRed
# of compounds
G
AcGFP/dsRed
# of compounds
H
Cells (2x10⁶)
of compounds

Figure 4.

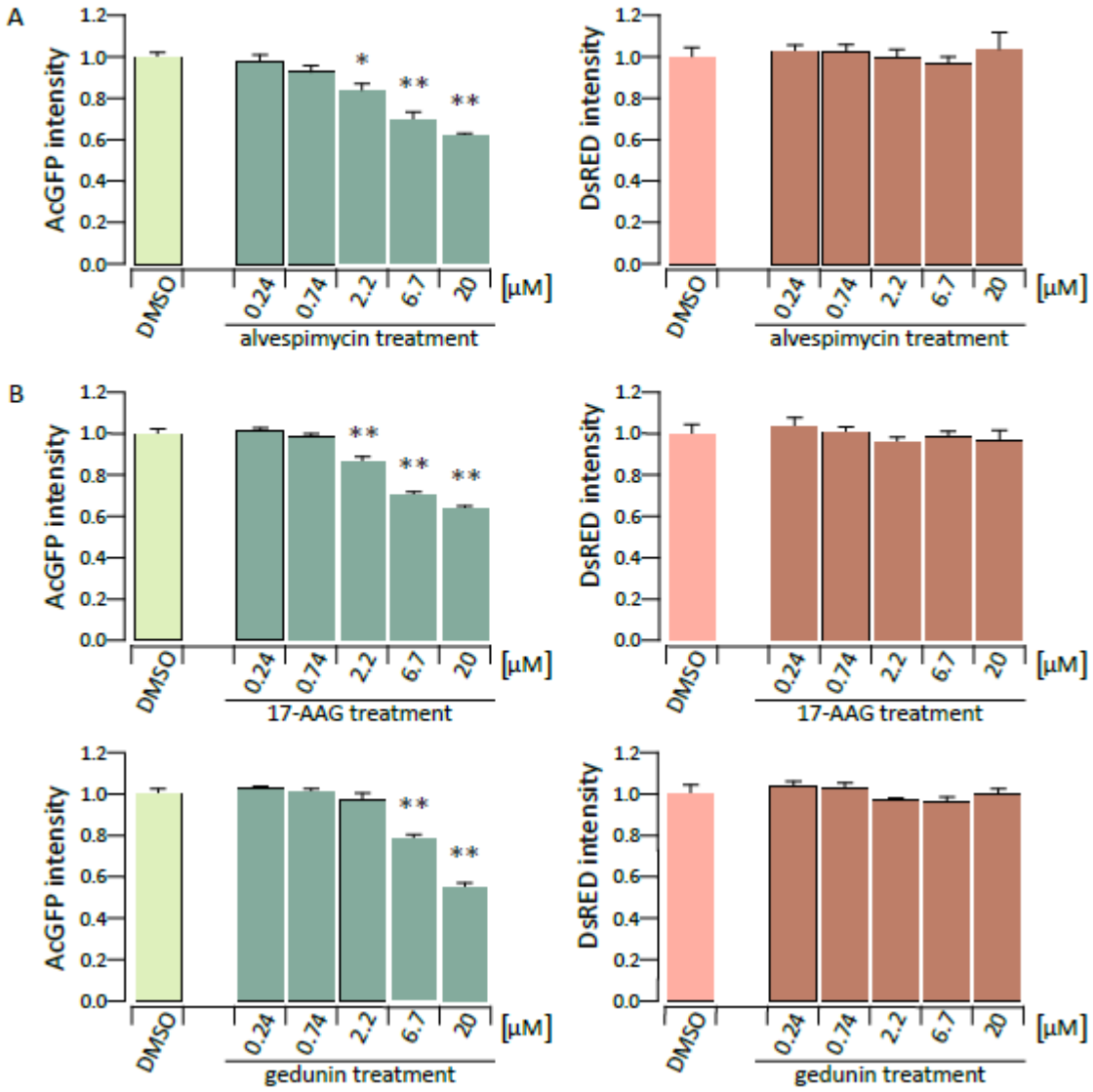
A
AcGFP intensity
DsRED intensity
1.2
1.0
0.8
0.6
0.4
0.2
0.0
*
**
**
DMSO
0.24
0.74
2.2
6.7
20
[µM]
alvespimycin treatment
B
17-AAG treatment
gedunin treatment

Figure 6.

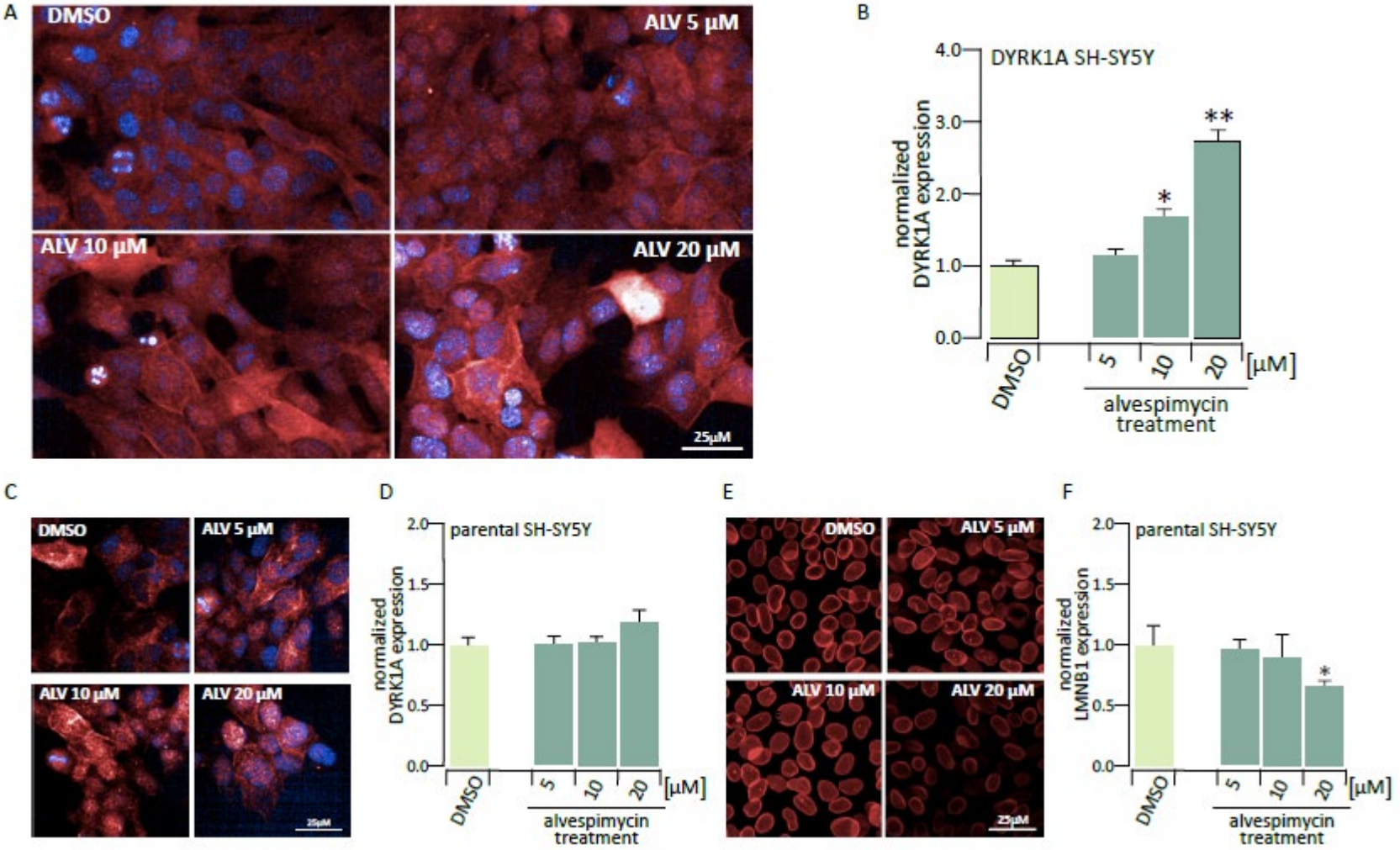
A
DMSO
ALV 5 µM
ALV 10 µM
ALV 20 µM
25µM
B
DYRK1A SH-SY5Y
normalized DYRK1A expression
4.0
3.0
2.0
1.0
0.0
*
**
DMSO
5
10
20
[µM]
alvespimycin treatment
C
DMSO
ALV 5 µM
ALV 10 µM
ALV 20 µM
25µM
D
parental SH-SY5Y
normalized DYRK1A expression
2.0
1.5
1.0
0.5
0.0
DMSO
5
10
20
[µM]
alvespimycin treatment
E
DMSO
ALV 5 µM
ALV 10 µM
ALV 20 µM
25µM
F
parental SH-SY5Y
normalized LMNB1 expression
2.0
1.5
1.0
0.5
0.0
*
DMSO
5
10
20
[µM]
alvespimycin treatment

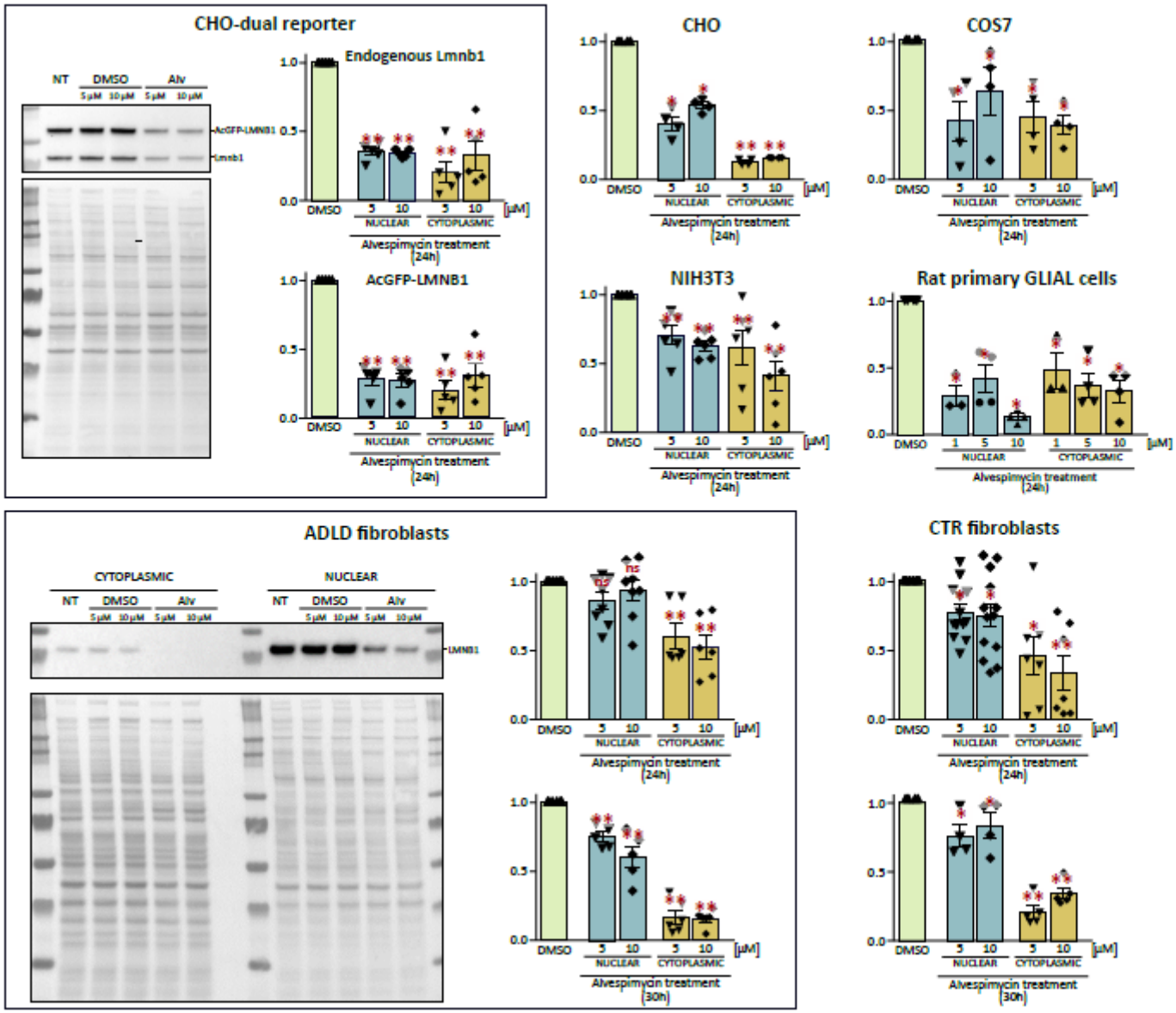
CHO-dual reporter
NT
DMSO
Alv
5 μM
10 μM
AcGFP-LMNB1
Lmnb1
Endogenous Lmnb1
AcGFP-LMNB1
DMSO
NUCLEAR
CYTOPLASMIC
[μM]
Alvespimycin treatment (24h)
CHO
COS7
NIH3T3
Rat primary GLIAL cells
ADLD fibroblasts
CYTOPLASMIC
NUCLEAR
LMNB1
ns
Alvespimycin treatment (30h)
CTR fibroblasts

Supplementary file.

Supplemental figure 1.

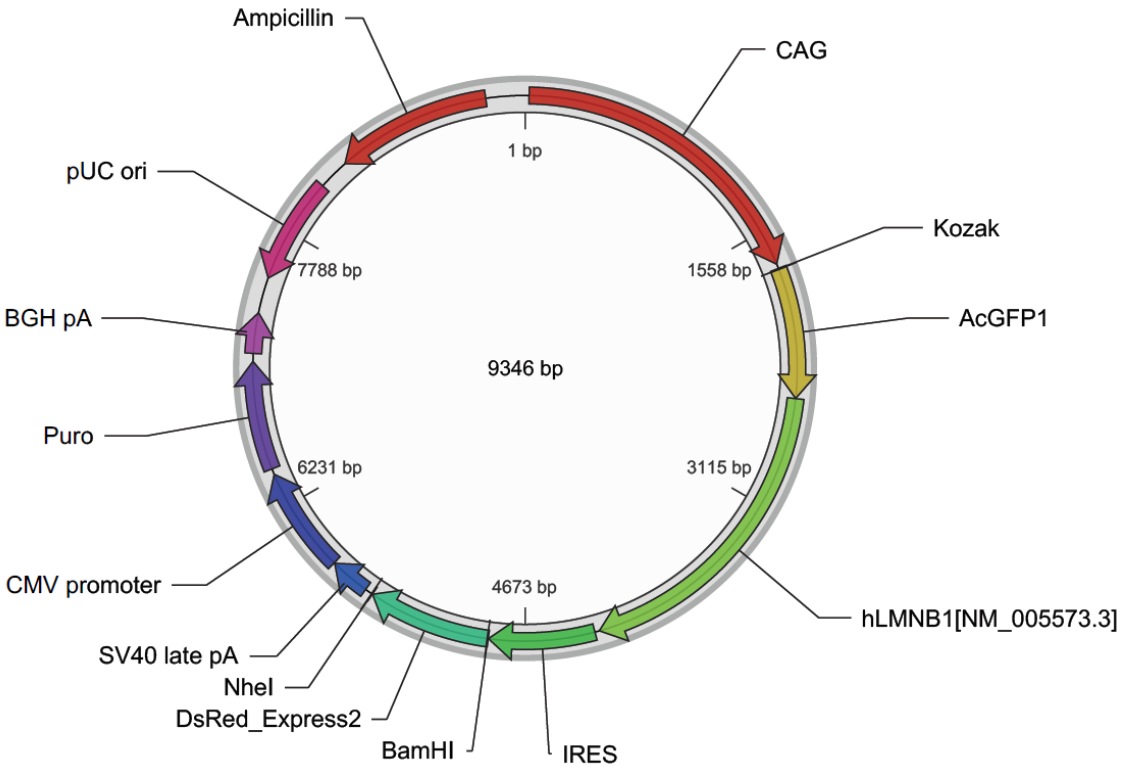

Supplemental figure 1. Schematic map of the *CAG-AcGFP1-hLMNB1-IRES-DsRed* plasmid.

Note: CAG: CAG eukaryotic expression promoter; AcGFP1: green fluorescent protein; hLMNB1: human Lamin B1 coding sequence; IRES: internal ribosomal entry site; DsRed_Express2: destabilized red fluorescent protein; SV40late pA: polyadenylation signal. The plasmid is puromycin and ampicillin resistant.